Clinical Studies Of Real-Time Monitoring Of Lithotripter Performance Using Passive Acoustic Sensors

T. G. Leighton[a], F. Fedele[b], A. J. Coleman[b], C. McCarthy[b], S. Ryves[c], A. M. Hurrell[d], A. De Stefano[e] and P. R. White[a]

[a]*Institute of Sound and Vibration Research, University of Southampton, Highfield, Southampton SO17 1BJ, UK (Corresponding author: tgl@soton.ac.uk)*
[b]*Medical Physics Department, Guy's and St Thomas' NHS Foundation Trust, Lambeth Palace Road, London SE1 7EH, UK.*
[c]*Stone Unit, Day Surgery Department, Guy's and St Thomas' NHS Foundation Trust, St Thomas Street, London SE1 9RT, UK.*
[d]*Precision Acoustics Ltd., Hampton Farm Business Park, Higher Bockhampton, Dorchester DT2 8QH, Dorset, UK.*
[e]*Radiological Science Group, Medical Physics Department, St Mary's Hospital, Portsmouth PO3 6AD, Hampshire, UK.*

Abstract. This paper describes the development and clinical testing of a passive device which monitors the passive acoustic emissions generated within the patient's body during Extracorporeal Shock Wave Lithotripsy (ESWL). Designed and clinically tested for use by a nurse, the device analyses the echoes generated in the body in response to each ESWL shock, and so gives real time shock-by-shock feedback on whether the stone was at the focus of the lithotripter , and if so whether the previous shock contributed to stone fragmentation when that shock reached the focus. A shock is defined as being 'effective' if these two conditions are satisfied. Not only can the device provide real-time feedback to the operator, but the trends in shock 'effectiveness' can inform treatment. In particular, at any time during the treatment (once a statistically significant number of shocks have been delivered), the percentage of shocks which were 'effective' provides a treatment score $TS(t)$ which reflects the effectiveness of the treatment up to that point. The $TS(t)$ figure is automatically delivered by the device without user intervention. Two clinical studies of the device were conducted, the ethics guidelines permitting only use of the value of $TS(t)$ obtained at the end of treatment (this value is termed the treatment score TS_0). The acoustically-derived treatment score was compared with the treatment score CTS_2 given by the consultant urologist at the three-week patient's follow-up appointment. In the first clinical study (phase 1), records could be compared for 30 out of the 118 patients originally recruited, and the results of phase 1 were used to refine the parameter values (the 'rules') with which the acoustic device provides its treatment score. These rules were tested in phase 2, for which records were compared for 49 of the 85 patients recruited. Considering just the phase 2 results (since the phase 1 data were used to draw up the 'rules' under which phase 2 operated), comparison of the opinion of the urologist at follow-up with the acoustically derived judgment, the correlation was good (kappa= 0.94), the device demonstrating a sensitivity of 91.7% (in that it correctly predicted 11 of the 12 treatments which the urologist stated had been 'successful' at the 3-week follow-up), and a specificity of 100% (in that it correctly predicted all of the 37 treatments which the urologist stated had been 'unsuccessful' at the 3-week follow-up). The 'gold standard' opinion of the urologist (CTS_2) correlated poorly

(kappa=0.38) with the end-of-treatment opinion of the radiographer (CTS_1). This is due to the limited resolution of the lithotripter X-Ray fluoroscopy system. If the results of phase 1 and phase 2 are pooled to form a dataset against which retrospectively to test the rules drawn up in phase 1, when compared with the gold standard CTS_2 , over the two clinical trials (79 patients) the device-derived scored (TS_0) correctly predicted the clinical effectiveness of the treatment for 78 for the 79 patients (the error occurred on a difficult patient with a high body mass index). In comparison, using the currently available technology the in-theatre clinician (the radiographer) provided a treatment score CTS_1 which correctly predicted the outcome of only 61 of the 79 therapies. In particular the passive acoustic device correctly predicted 18 of the 19 treatments that were successful (i.e. 94.7 sensitivity), whilst the current technology enabled the in-theatre radiographer to predict only 7 of the 19 successful treatments (i.e. 36.8 sensitivity). The real-time capabilities of the device were used in a preliminary examination of the effect of ventilation.

Keywords: Lithotripsy, Cavitation, Kidney stone fragmentation, ESWL, passive acoustic sensor.
PACS: 43.20.Fn, 43.25.Cb, 43.25.Vt, 43.25.Yw, 43.25.Zx, 43.30.Lz, 43.35.Ei, 43.35.Hl, 43.35.Yb, 43.60.Lq, 43.80.Ev, 43.80.Gx, 43.80.Qf, 43.80.Sh, 43.80.Vj, 87.50.yt.

INTRODUCTION

Background

In the earlier 1990's Leighton and Coleman identified a two-burst structure (Fig. 1) present in the time histories of the passive acoustic emissions detected during lithotripsy, and by comparing this structure with the time histories of sonoluminescent emissions, identified the two bursts as relating to cavitational collapses [1-3].

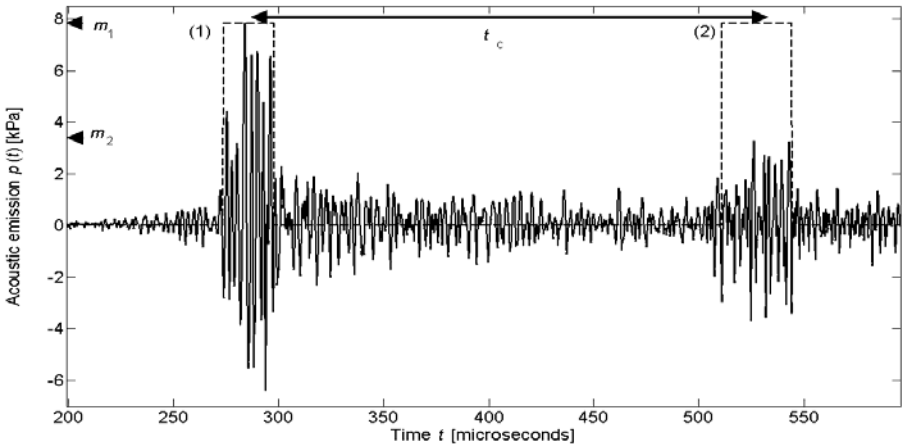

FIGURE 1. Example of the time domain analysis of an *in vivo* signal. The dashed boxes indicate those two portions of the signals that are attributed to the (1) first and (2) second bursts. The two bursts are separated by a collapse time t_c= 246 μs and each of these bursts is then characterised in terms of a maximum amplitude (m_1 = 7.8 kPa and m_2 = 3.3 kPa respectively) [9-13]. The method of calculating these values is discussed in reference [13]. This trace was recorded using one of the clinical prototypes developed in this study (Mark III), and a signal conditioning system that includes a high pass filter at 300 kHz and a preamplifier. The data acquisition system is described in details in Fedele [11].

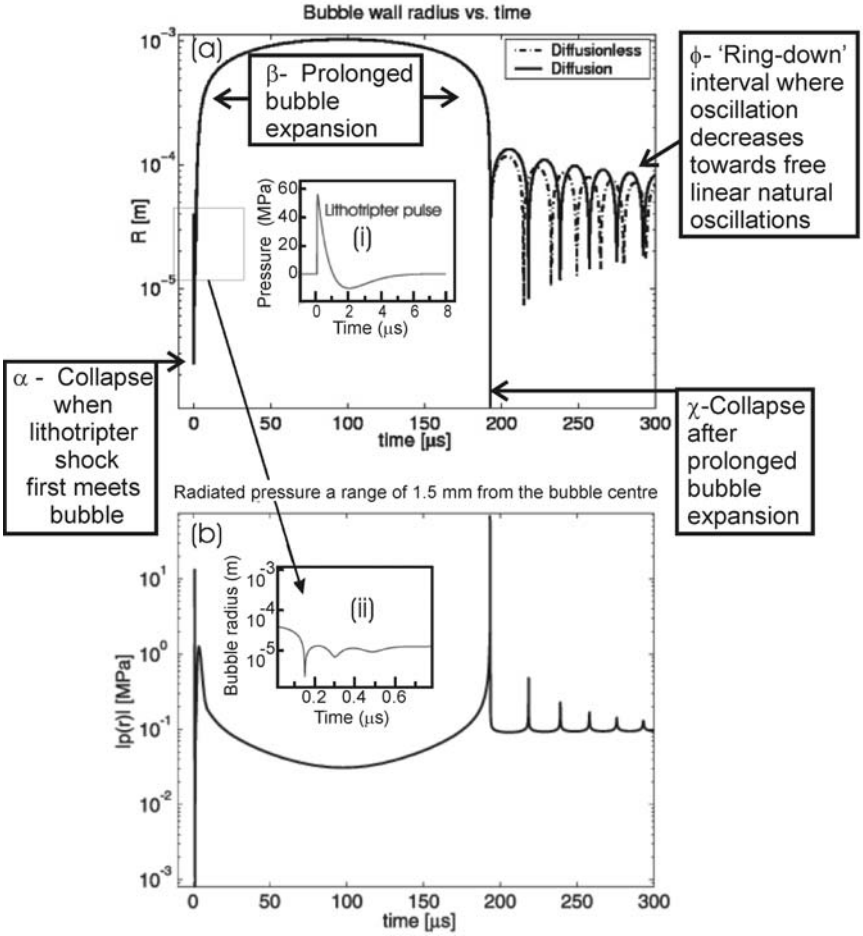

FIGURE 2. An air bubble of initial radius 40 microns in water is subjected in the free field to the lithotripter pulse shown in inset (i) (Peak positive pressure = 56 MPa; Peak negative pressure = -10 MPa). (a) The bubble radius time history, as predicted by the Gilmore model, is shown for conditions with (solid line) and without (dashed line) mass flux across the bubble wall. Note that the inclusion of diffusion makes the final bubble size greater than the initial size, with a consequent slight decrease in the period of the oscillations (i.e. a reduction in the frequency) at the timescales marked ϕ. Inset (ii) shows the micro-rebounds that are visible in the fine detail of the collapse which occurs around t=0. Similar features are seen in the CFD predictions (Turangan *et al.* [7]). (b) On a common time axis with (a) and for the same bubble collapse, the pressure that would be measured 1.5 mm away from the bubble centre is shown. Two main emissions (at $t \approx 0$ μs and at $t \approx 190$ μs) are associated with rebounds in (a), subsequent emissions being smaller. The overall effect of such pairs of emissions from the collapse of a cloud of bubbles was identified as demarcating the interval t_c in the early 1990s [1-3]. Comparison of (a) with (b) suggests that the source of the first peak is the cavitational collapse which results when the lithotripter first meets the bubble (label α). After this collapse, the Gilmore model suggests that the bubble undertakes a prolonged expansion phase (label β), before collapsing again (at which time the second peak in acoustic emission and luminescence is generated; label χ). The bubble must remain spherical and intact in the Gilmore model, so that after this second collapse the bubble oscillates with gradually decreasing amplitude, with a frequency which tends ever more closely to its 'Minnaert' frequency as time proceeds (label ϕ).

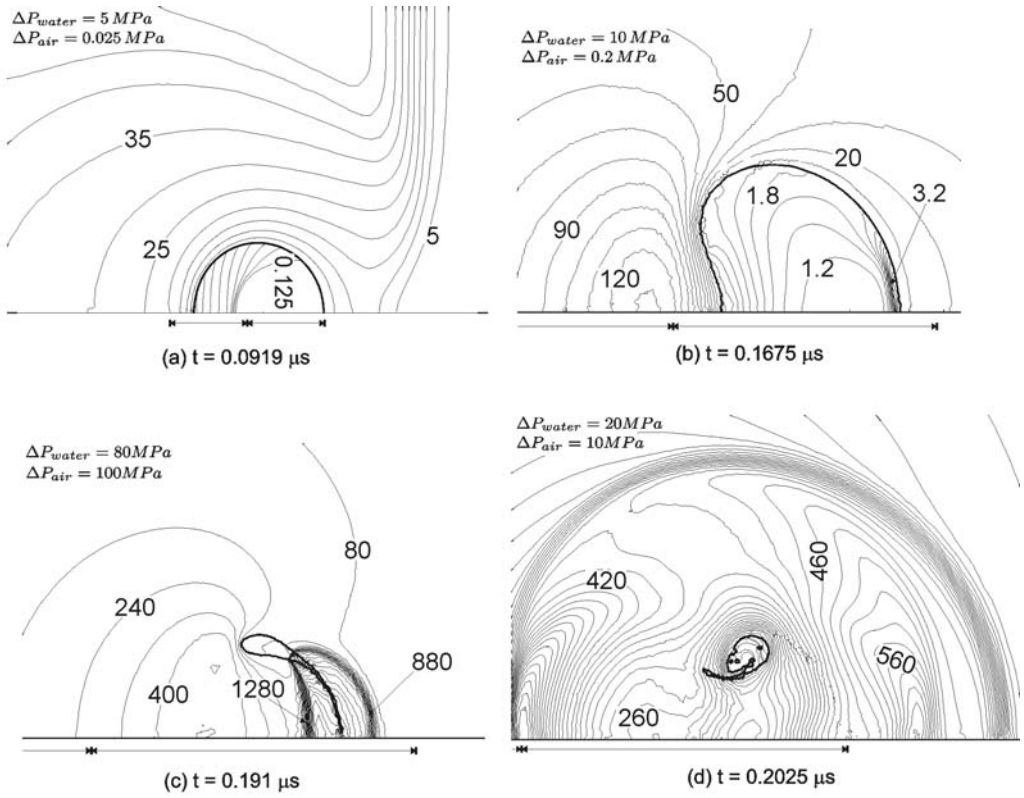

FIGURE 3. An air bubble of initial radius 40 microns in water is subjected in the free field to a lithotripter pulse (propagating from left to right). The axis of rotational symmetry is the horizontal line at the base of each plot. The contour increments in pressure for both air and water are indicated on each plot, the value of selected contours being labelled in MPa. All elapsed times 't' are measured after the lithotripter pulse first meets the upstream bubble wall. (a) The lithotripter pulse has passed over the bubble, travelling further than the slower gas shock within the bubble. An expansion wave is reflected back off the bubble, travelling to the left and upwards in the picture. (b) The bubble involutes as it collapses, to form a liquid jet which will pass through the centre of the bubble. (c) The impact of the jet against the downstream bubble wall generates a blast wave, which propagates outwards in (d). Such liquid impacts and blast waves can generate erosion and biomechanical effects. The high temperatures and pressures attained within the gas can generate chemical effects and luminescence. Movies of this CFD code in operation can be found at the online page associated with the paper [7]: http://journals.cambridge.org/fulltext_content/supplementary/S0022112007009317sup001/index.html
Figure reproduced from reference [5].

Furthermore, through use of the Gilmore equation (Fig. 2), they identified the time interval between the two bursts (t_c) as corresponding to the period of prolonged expansion between two cavitational collapses: the first collapse occurs when the shock wave from the lithotripter first impacts upon the bubble, and the second collapse occurs over 100 μs later. Using the Gilmore equation, they showed that t_c depended on the initial bubble size and the strength of the lithotripter shock wave, and provided experimental evidence for this [1-4]. Finally, they discussed the possibility that such

passive acoustic emissions could be used to monitor the efficacy of lithotripsy treatments in real-time [1-3].

To bring such a concept to fruition required improvements in the simulation capability, since the Gilmore model contains limiting assumptions, most notably that the bubble remains spherical at all times. Alternative methods, which allow for the departure of the bubble wall from sphericity, could not model the blast wave produced when the bubble collapses [5-8]. This blast wave is a vital feature, since the GPa pressures in the diverging blast wave (Fig. 3) exceed by two orders of magnitude the compressive pressure in the lithotripter shock wave, and so failure to incorporate them in the model neglects what is potentially a significant contributor both to the far field acoustic emissions and to the stone fragmentation (bearing in mind the differing geometric spreading characteristics of the two waves). Hence a free-Lagrange computational fluid dynamics (CFD) scheme was developed for simulating bubble collapses during ESWL, initially in free field (Fig. 3) [5, 6] but then incorporating multiple bubbles, bubble cloud effects, the presence of solids in the vicinity of the stone, and the effect of the geometry of that solid on the pressures and stresses induced. The method is outlined in reference [7], with later papers in preparation detailing the multi-bubble stages of the CFD and the far field predictions of the emissions.

In parallel with these CFD studies (and informed by them) a programme of *in vitro* tests were conducted in order to progress towards the design of the hardware, software, and rules for the operation of the passive acoustic device for in-theatre real-time monitoring of ESWL [9-12]. These rules were important, since the most challenging component in this study was to condense the myriad of complicated interactions between shock, tissue, stone and bubble into two simple, reliable, and easily observable parameters (m_2/m_1 and t_c; see Fig. 1) which could be judged against preset rules in order to assess, in real time, whether each shock delivered to the patient in a given ESWL treatment session was 'effective' [13]. By 'effective', we mean that the shock was (i) on-target, in that the stone was appropriately in the focus of the ESWL device; and (ii) that the shock effectively contributed to the fragmentation of the stone.

Condensing the interpretation of the passive acoustic emissions into two parameters (m_2/m_1 and t_c), despite the myriad sources which can contribute to those interactions, was a considerable task. The simplified explanation for the two-burst structure given above has appealed to idealized descriptions of single-bubble cavitation, and very simplified concepts of scattering from the stone. Since its discovery [1], a range of authors exploited this two-burst structure in ingenious ways [14-17]. One might therefore ask whether the device outlined in this paper relies on cavitation being the major cause of stone fragmentation in order to operate effectively. The answer to this question is no. The cavitational interpretation of the passive acoustic emission was used as a starting point, acting rather as the first 'stepping stone' rather than a 'bridge' between the concept of this device and the implementation of this device in the clinic.

Coleman *et al.* [1] had access to a narrow-band passive acoustic detector, but proposed that use of a wide-band receiver might detect useful resonances. Prior to the clinical trials, the research effort investigated both the information that was available in the time-history of the passive acoustic emissions, and also the information available in the spectral representation (Fig. 4), and the time-frequency representation (Fig. 5). Data was taken both *in vitro* and *in vivo* [4, 9-11, 21].

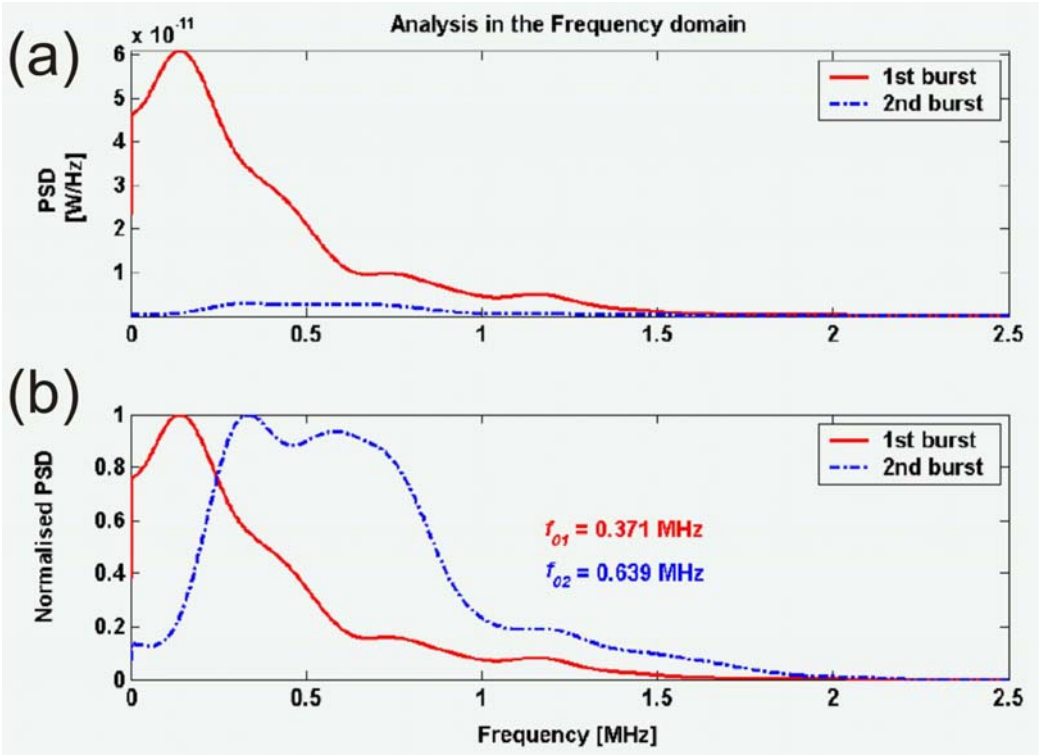

FIGURE 4. Example of frequency analysis of the content of the two bursts obtained *in vitro* from tap water, shown with same absolute reference in (a), but in (b) the same data is shown with the spectra of each burst has been normalised to the peak for that burst (effectively increasing the gain for the second burst data). The data were taken prior to the development of the final prototype sensor used in the clinical trials, using a sensor developed at the UK National Physical Laboratory (see [11] for details). With these data the algorithm (Fedele [11]) for detecting the central frequency for the first burst gives an answer of f_{01} =0.371 MHz, and for the central frequency of the second burst it provides f_{02} =0.639 MHz. However such analysis needs to be treated with caution, as the calculated frequencies can be strongly influenced by factors not present in the raw data (see text). Figure reproduced from Fedele *et al.*, 2004 [21]. For further details see Fedele [11].

Although the spectral characteristics of the passive acoustic emissions were investigated as a way of providing a diagnostic of stone fragmentation, and initially provided promising results [9-11, 20, 21], they proved to be a significantly less reliable method *in vivo* for the device built for this study than was characterization using the time history (see below). It is important to emphasize that this does not

imply that a different device, designed specifically for spectral characterisation *in vivo*, might not provide useful information. Owen *et al*. [18] have through careful experimentation exploited the spectral characteristics of such passive acoustic emissions successfully to distinguish *in vitro* between complete and dissected glass spheres at the focus of a lithotripter, and tracked changes in model stone size [19].

The problems encountered with the device of the current study, and which a device designed to exploit spectral characteristics *in vivo* should be designed to counter, are as follows.

Consider Fig. 4. Whilst the prototype transducer for use in the clinical trials was being developed, a range of earlier prototypes and other sensors were tested to inform the design process. The data of Fig. 4 were taken in tap water using a sensor developed by the UK National Physical Laboratory, which was positioned so as to be primarily sensitive to the region at the lithotripter focus. An algorithm readily provides estimates for the central frequencies of the first and second bursts (f_{01} and f_{02} respectively). However such analysis needs to be treated with caution. To prevent the EM noise from the lithotripter source from dominating the signal, a 200 kHz high-pass filter was used. The peak for the first burst in Fig. 4 is below this frequency, so that the central frequency calculated from these data for the first burst will be strongly influenced by the characteristics of the filter.

The spectrum of the second burst appears to show considerable frequency content above the 200 kHz setting of the high pass filter. A weighted average of the energy in this burst provides a sensible estimate for f_{02}. However when such a procedure was attempted *in vivo*, the signal-to-noise ratio above ~500 kHz was significantly reduced, so that the calculated value of f_{02} became heavily dependent upon the upper frequency limit chosen for the averaging [11].

Artificial factors such as these tend to become more problematic (for both the first and second burst) as the signal-to-noise ratio deteriorates, and therefore it was not unsurprising that *in vivo* the spectral characteristics proved to be less useful in discrimination than did the temporal ones for our device. Even *in vitro*, when faced with asymmetric mineral shapes, the initially promising spectral discrimination [11, 20] showed less promise than did the time history in being reduced to simple parameters for an automated system to use [9, 10, 20, 21]. For example, the trends in the central frequencies in Fig. 6(a) are less significant (when the uncertainties in the error bars are taken into account) than the trends in the time histories for the same data (Fig. 6(b)). Therefore the clinical studies were based on parameterization of the time histories rather than the spectral information (recalling however that this does not imply that devices specifically designed to rely on spectral information *in vivo* may not prove to be effective [18, 19]).

The remainder of the paper will therefore describe how three automated measurements of the time history were reduced to two parameters to allow automated diagnosis.

(a)

(b)

(c)

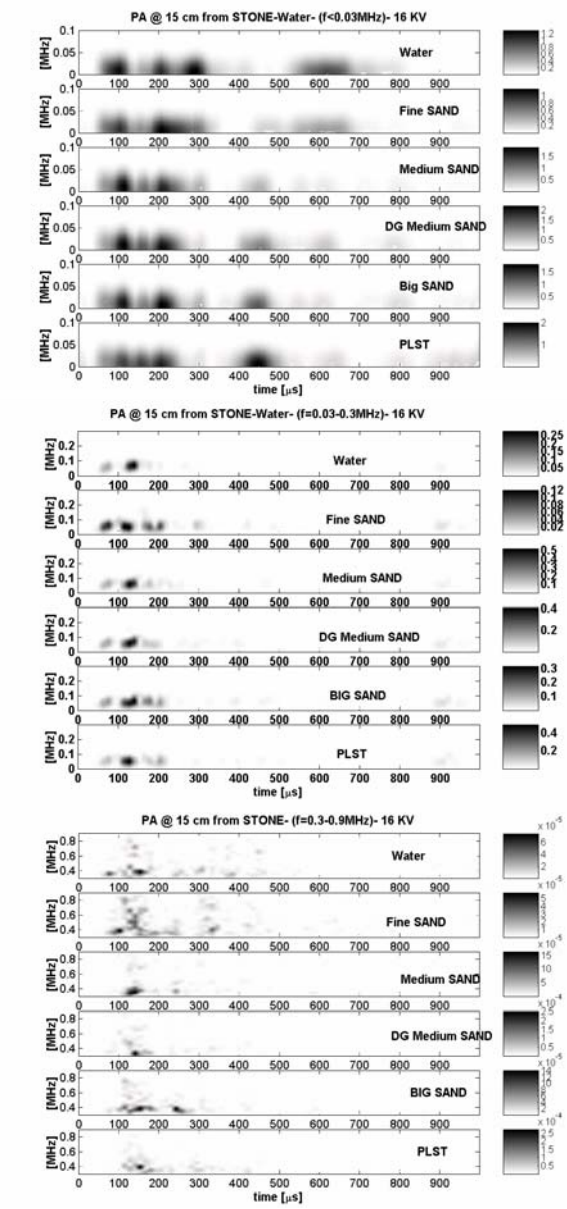

FIGURE 5. Example representation of passive signals in time-frequency representation for (a) very low frequency (VLF, <30 kHz); (b) low frequency (LF, 30-300 kHz); and (c) high frequency (HF, 300-900 kHz) bands. The six subplots within (a), (b) and (c) represent *in vitro* scatter from different target materials, using equal volumes of each (33.5 ml), and consisting of (from the bottom upwards, with fragments sizes selected sieves) of: PLST (Plaster of Paris made using a ratio plaster:water of 2:1 and injected into the target holder in the liquid state by a syringe avoiding air entrainment); Big sand (diameters of 10-30 mm); Medium sand (diameters of 4-10 mm, where DG implies the degassed samples – all other samples are immersed in tap water); Fine sand (diameters of 1- 4 mm). Figure reproduced from Leighton *et al.*, 2004 [20]. The data were recorded using one of the prototype clinical sensors developed in this study (Mark I, [11]). The raw data were filtered digitally using Butterworth filters. For further details see Fedele [11].

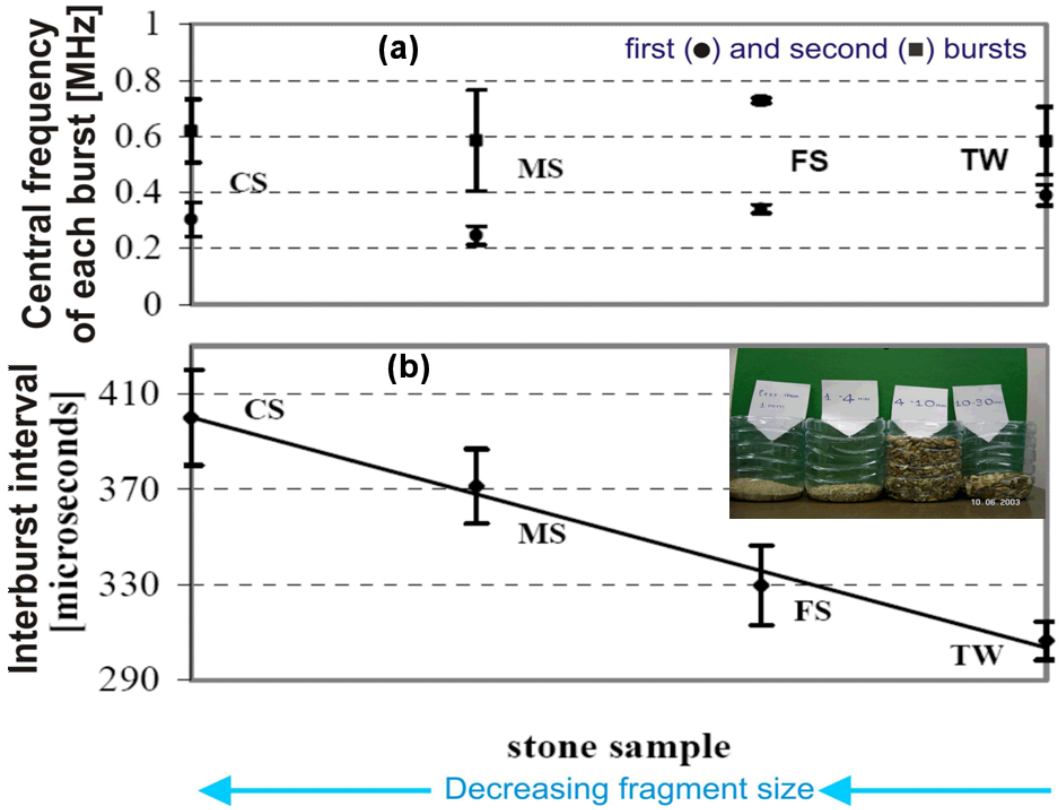

FIGURE 6. Example of the variation with mineral particle size of the central frequencies of the first (f_{01}) and second (f_{02}) bursts, taken with the Mk 1 prototype and a 200 kHz high pass filter (see Fedele [11] for details). A ping-pong ball sample holder contained tap-water (TW), or various samples of stone. Samples of the latter are shown in the inset to part (b) in the following order, from left to right: a very fine sand sample with grain diameter of less than 1 mm is shown on the far left; second from the left is fine sand (FS, grain diameter 1-4 mm); second from the right is medium sand (MS; grain diameter 4-10 mm); on the far right is coarse sand (CS; grain diameter 10-30 mm). Figure reproduced from Fedele *et al.*, 2004 [10, 21]. For further details see Fedele [11].

Aims and Objectives

To summarise, the goal of this project was to develop a passive 'listening device' (in the form of a single sensor transducer, for simplicity and to minimize cost) which can report, in real-time, the 'effectiveness' of each shock during ESWL, where the 'effectiveness' is judged on two points:

(i) Is the shock on-target (i.e. hitting the stone)?

(ii) Did the shock contribute to stone fragmentation?

Our Ethics permission forbade us from providing operator with any information (in case it altered treatment, or skewed results). Hence the following longer-term objectives could not be included in this study:

- To provide an alternative to using a preset number of shocks;
- To alert operator in real time to the possible need to check targeting;

- To reduce morbidity by reducing exposure to minimum required;
- To reduce retreatment rates (currently at 30-50%).

Given these restrictions, although the device does provide real-time feedback, the ethics permission only allowed us to compare the end-of-treatment score automatically generated by the acoustic system (TS_0) with the treatment score provided by the consultant urologist at the three-week follow-up appointment (CTS_2).

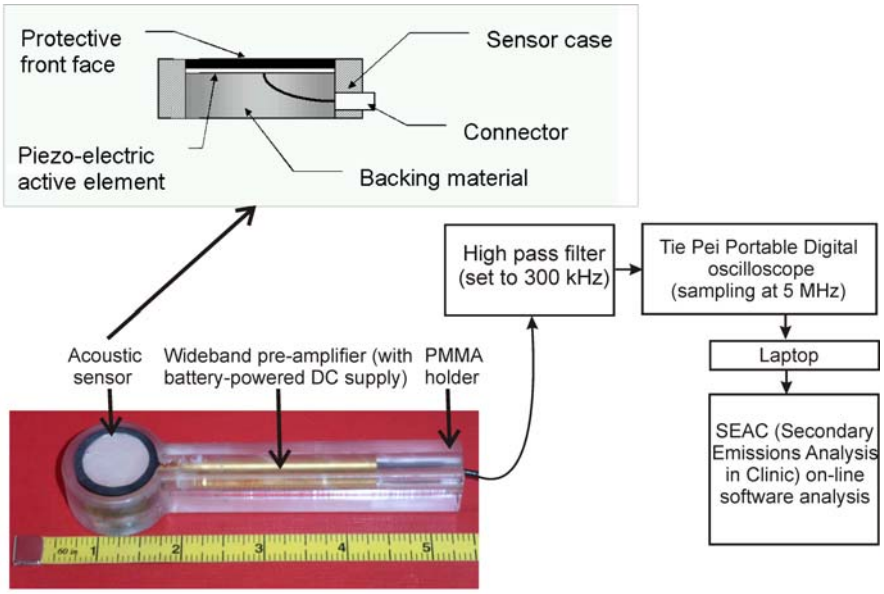

FIGURE 7. Schematic of the apparatus. The signal from the transducer and pre-amplifier (manufactured by Precision Acoustics Ltd.) is high-pass filtered to reduce noise and captured by a portable oscilloscope before being analysed on the laptop using the SEAC (Secondary Emissions Analysis in Clinic) on-line software (see Fig. 13). Figure reproduced with permission from reference [13], where it previously appeared: *Ultrasound in Medicine and Biology* doi:10.1016/j.ultrasmedbio.2008.03.011 in press (by T. G. Leighton, F. Fedele, A. J. Coleman, C. McCarthy, S. Ryves, A. M. Hurrell, A. de Stefano, and P. R. White) "A device for monitoring the efficacy of ESWL using passive acoustic emissions, Copyright Elsevier 2008.

METHODS

Two clinical trials of the device were undertaken (named 'phase 1' and 'phase 2'). [13]. In preparation for these, extensive development stages were conducted. These included the development of the hardware (Fig. 7). Informed by input from the CFD simulations [5-7, 12], the preparatory stages before the two clinical trials also included the testing of the method *in vitro* and on 51 test subjects *in vivo* [9-12].

The decision as to whether a shock is 'effective' or not, is based on a set of 'rules' (Fig. 8). The process by which these rules were derived was detailed elsewhere [9-13]. However a simplified explanation is outlined schematically in Figs. 9 and 10, and will

now be described. Bear in mind the comments in the 'Background' section that, whilst this simplified explanation of the rules relies on a cavitational interpretation, this does not mean that for the device to work, cavitation must be the dominant mechanism for stone fragmentation.

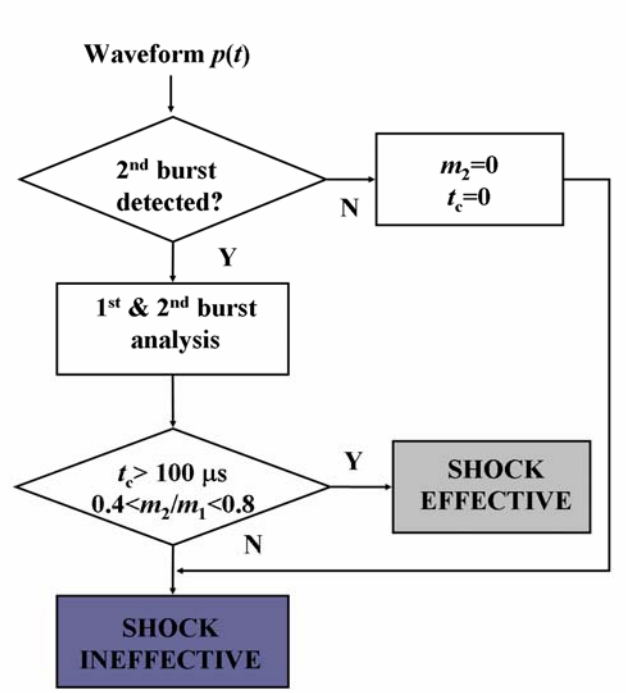

FIGURE 8. A block-diagram of the Secondary Emissions Analysis (SEAC) software. The detected acoustic emission is processed, making use of clinically derived data on the acoustic parameters m_2 / m_1 and t_c, to generate an indication to the operator of the 'effectiveness' of a shock (the 'rules' displayed in the lower diamond correspond to those determined by phase 1 for use in phase 2). Figure reproduced with permission from reference [13], where it previously appeared: *Ultrasound in Medicine and Biology* doi:10.1016/j.ultrasmedbio.2008.03.011 in press (by T. G. Leighton, F. Fedele, A. J. Coleman, C. McCarthy, S. Ryves, A. M. Hurrell, A. de Stefano, and P. R. White) "A device for monitoring the efficacy of ESWL using passive acoustic emissions, Copyright Elsevier 2008.

Fig. 9 illustrates a simple interpretation of the two-burst structure outlined in the Introduction. An amplitude m_1 is assigned to the first burst (the temporal peak within the burst is chosen, although a pulse average system could also be used). The inter-burst period t_c (calculated through a weighted function described in reference [13]) corresponds to the collective prolonged expansion phases of the bubble cloud, after which comes the second burst which has an amplitude m_2. High values of both t_c and m_2 could be taken to indicate strong cavitation, whilst weak cavitation would produce low values of both. The first burst contains components both of the reflection of the incident lithotripter shock wave from the stone, information about the waves which propagate within the stone as a result of ESWL, and cavitation: if, for example the

lithotripter shock wave were to miss the stone, a reduction in the reflection component would reduce the value of m_1 (in the same way in which, if a railway worker hits a hammer against the wheel of a locomotive to test for its integrity through its passive emissions, no such emissions are generated if the worker misses the wheel with the hammer - although of course when lithotripter shocks are projected into the body, other scattering sources contribute to m_1 when the stone is not at the focus).

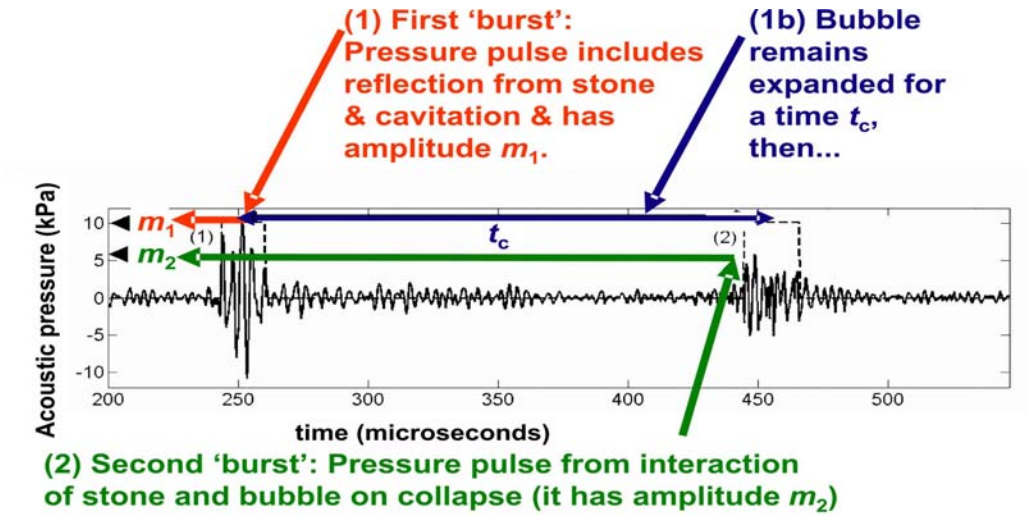

FIGURE 9. Simplified interpretation of a time-history of the detected passive emissions. This emission was recorded *in vivo* using the final clinical prototype (Mark III), and the conditioning system developed in this study. The clinical data acquisition system (that includes the sensor Mark III, a high pass filter at 300 kHz and a preamplifier) is described in reference [11].

Fig. 10 shows how the simple interpretation of the time history (Fig. 9) can be used to make simplistic predictions about the factors which influence the values of m_1, m_2 and t_c recorded in response to each lithotripter shock wave. To normalize the amplitude results to account for differing sizes of patients, different lithotripter energy levels and coupling efficiencies, the ratio m_2 / m_1 is calculated for each shock echo, and this ratio is plotted against t_c. In this way, in real time as each ESWL shock is delivered during a treatment, a point is added to the plot of m_2 / m_1 against t_c: if that point falls within a box (the 'strike zone', as shown by the dotted lines on Fig. 10), then the shock is taken to have been 'effective'. However if the point falls out of the 'strike zone', the shock is taken to be 'ineffective'.

In this way, the system builds up a real-time picture of how the treatment is progressing. In this idealized scheme, if for example the stone moved out of the focus, the value of m_1 would fall because of the reduction in the reflected component of the incident shock wave. This would cause an increase in m_2 / m_1 and the point would fall above the 'strike zone' (as indicated for many of the points in Fig. 10). In an alternative scenario, if weak cavitation occurred, both m_2 and t_c would decrease, such that the points would ideally fall below and to the left of the 'strike zone'. If the

algorithm fails to detect two distinct bursts in the echo, then both m_2 / m_1 and t_c are conventionally equalled to zero, and a point is placed on the origin of the graph shown schematically in Fig. 10 (see reference [13] for details).

Having established the principle that an 'effective' shock would result in an echo placed within a 'strike zone' drawn on a graph of m_2 / m_1 against t_c, and an 'ineffective' would result in an echo placed outside of this box, the two clinical studies (phase 1 and phase 2) were undertaken.

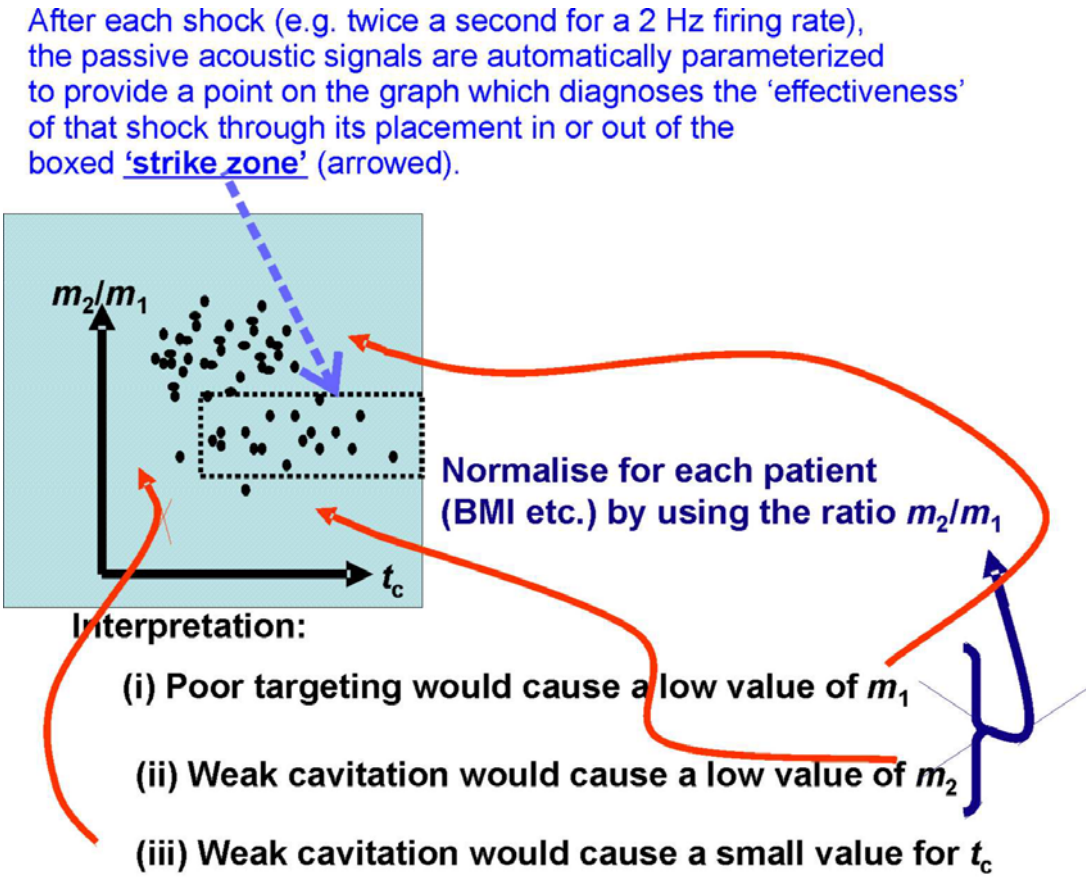

FIGURE 10. Simplified interpretation of how the physical parameters affect the placing of the points (parameterized in terms of m_1, m_2 and t_c) recorded after each ESWL shock (assumed to be acquired two a second for an assumed 2 Hz firing rate). The curved arrows (shown red in the colour version) indicate idealized scenarios (described in the text) through which the points might fall outside of the box (the 'strike zone', shown by dashed lines), indicating that these were 'ineffective' shocks (see text). Readers should note that this is a simplification and are directed to reference [7] for a more rigorous description.

CLINICAL STUDIES

The two clinical studies reported in this paper were carried out by the Medical Physics Department at Guy's & St Thomas' NHS Trust, London on patients treated for stones either in the renal pelvis or the calicies on Storz Modulith SLX lithotripter (Storz Medical AG, Tägerwilen, Switzerland) located in the Stone Unit of the same Trust. The studies received ethics approval and the first study (phase 1) commenced in April 2006 and, together with the phase 2 study, lasted 15 months. The scope of the ethics approval did not allow the ESWL operator to alter the treatments in any way in response to information provided by the output of the passive acoustic device. The study aim was confined, therefore, to examining the correlation between the acoustic data and the clinical outcome. The object of the phase 1 study was to build on the *in vitro* and CFD results to finalise the rules for determining the effectiveness of each shock. In phase 2, these rules were implemented and the system was validated.

A total of 118 patients consented to take part in phase 1. Shock-by-shock sequences of acoustic data from the sensor were retained for the analysis of each treatment. A clinical follow-up three weeks after treatment was obtained for 67 of these subjects in phase 1 (of the remainder, 18 subjects could not tolerate the procedure, for 3 patients the pre-treatment and post-treatment X-Rays were not of adequate quality for reporting, and in 30 further cases the patients failed to return for the follow-up appointment). The acoustic data from these 67 subjects were examined, and a further 37 of these subjects were excluded on the basis that the recorded sequences of the patient in question represented less than 30% of the shocks administered to that patient during the treatment session (phase 1 was used not only to test the 'rules' for the diagnosis, but also to test and enhance the ruggedness of the hardware and software and the procedure by which the nurse recorded ancillary data – such as the lithotripter setting – during the treatment). The remaining 30 subjects constituted the group retained for phase 1 analysis. This high recruitment attrition rate reflected, as explained above, a relatively high incidence of equipment issues early on in the study as well as administrative difficulties in getting X-rays reported. The final group of 30 subjects had an average ($\pm$ 2 standard deviations) of 2473 ± 1204 shocks administered during treatment using the Storz Modulith. Energy settings from 1 to 6 were used.

A total of 85 patients were recruited to phase 2, of which 49 satisfied the two conditions required for their acoustic data to be included in the trial: firstly, a complete clinical follow-up at three weeks was available; and, secondly, the recorded sequences for each patient represented at least 30% of shocks given to that patient during the treatment session. The attrition rate in phase 2 was considerably better than in phase 1 owing to improved experience with the passive acoustic system. To be specific, treatment was not tolerated by 3 patients, no follow-up was available for 16 patients, and in a further 2 cases the X-rays were of poor quality and could not be interpreted. The equipment was damaged for 15 cases.

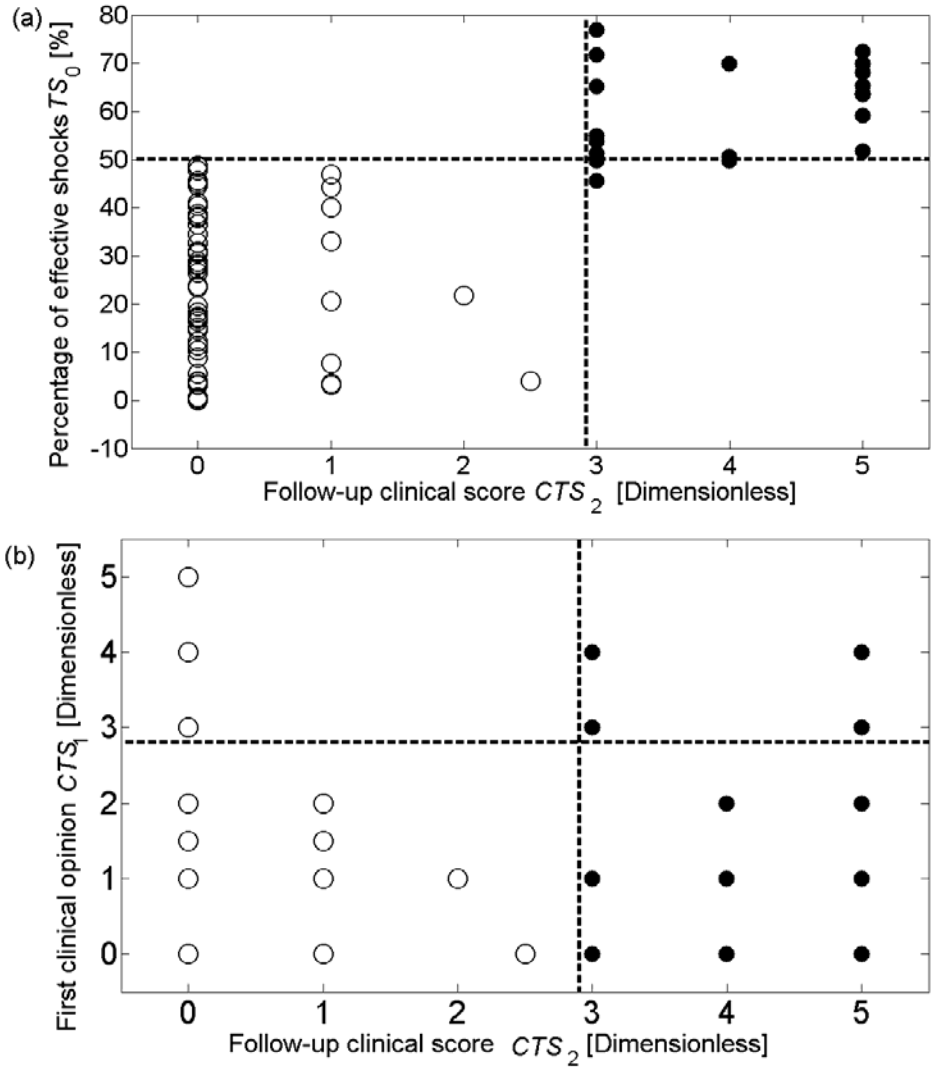

FIGURE 11. The combined results of the phase1 and phase 2 clinical studies. Each point represents a single treatment. The abscissa of both plots (a) and (b) indicates the CTS_2 score, the 'gold standard' provided by the urologist at the three-week follow-up. Using this gold standard, the solid circles indicate 'successful' treatments (i.e. $CTS_2 \geq 3$) and the open circles indicate 'unsuccessful' treatments (i.e. $CTS_2 < 3$), a vertical dashed line showing this demarcation. Both plots contain 79 points, although fewer are visible in (b) because the quantization of the scoring generates overlaps (two patients score $CTS_1 = 3$ with $CTS_2 = 5$; two patients score $CTS_1 = 3$ with $CTS_2 = 0$; three patients score $CTS_1 = 4$, $CTS_2 = 5$; four patients score $CTS_1 = 2$ with $CTS_2 = 0$; four patients score $CTS_1 = 1$ with $CTS_2 = 1$; five patients score $CTS_1 = 1$ with $CTS_2 = 3$; thirteen patients score $CTS_1 = 1$ with $CTS_2 = 0$; twenty-nine patients score $CTS_1 = CTS_2 = 0$). Plot (a) compares the treatment score from the acoustic device (TS_0) with CTS_2. The horizontal dashed line indicates the $TS_0 \geq 50\%$ delineator. Plot (b) does a similar comparison against CTS_2, but this time for the radiographer's initial clinical treatment score, CTS_1. The horizontal line in (b) distinguishes the radiographer's estimate of 'successful' treatments (i.e. $CTS_1 \geq 3$) from the radiographer's assessment of an 'unsuccessful' treatment (i.e. $CTS_1 < 3$). See reference [13] for details of the individual phases which are combined to generate this plot.

The average number of shocks administered in the phase 2 group was similar to that in phase 1, at 2461 ± 1160. Energy settings from 1 to 6 were used. The operators favoured setting 4 for the majority of treatments in both phase 1 and 2, although some variation occurred in all cases at the start and following realignment of the stone and in some cases higher settings were used.

Leighton *et al*. [13] analyze the results of the two clinical phases separately. This is the appropriate method since the results of phase 1 are used to define the rules, and the results of phase 2 are used to test the rules. For this paper the authors were asked that the data from the two phases be presented in a combined plot, rather than presenting the data from the two phases separately. This is done in Fig. 11. However it is noted that Fig. 11(a) does include an element of circular argument, since use of the plot to test the effectiveness of the rules would include some of the data that were used to draw up those rules. Readers wishing to see the separate plots are directed to Leighton *et al*. [13].

Fig. 11(a) indicates that the clinical trials showed the acoustic device to be successful. It plots the device-derived scored, TS_0 (which is given by the percentage of shocks that lay within the strike zone at the end of treatment) against the gold standard treatment score, CTS_2 (detailed in the following subsection). Compared with the gold standard CTS_2, over the two clinical trials (79 patients) the device-derived scored (TS_0) correctly predicted the clinical effectiveness of the treatment for 78 for the 79 patients (the error occurred on a difficult patient with a high body mass index). In comparison, using the current available technology the in-theatre clinician (the radiographer) provided a treatment score CTS_1 which correctly predicted the outcome of only 61 of the 79 therapies (Fig. 11(b)). In particular the passive acoustic device correctly predicted 18 of the 19 treatments that were successful (i.e. 94.7 sensitivity), whilst the current technology enabled the in-theatre clinician to predict only 7 of the 19 successful treatments (i.e. 36.8 sensitivity).

Details of the conduct and results of the separate Phase 1 and Phase 2 clinical studies (including details of how CTS_1 and CTS_2 were attained) are provided in the following subsections.

Phase 1 clinical study

In addition to the testing of the hardware, the software and the procedures described above, there were two main goals for the phase 1 study. Both of these goals refer to providing the device with the ability automatically to estimate the success of a treatment (either at the end-of-treatment (TS_0), or during treatment when a significant proportion of shocks have been delivered ($TS(t)$)). They are described below.

The first goal of phase 1 was to define the limits of the strike zone for *in vivo* data. The appropriate limits to define the 'strike zone' for *in vitro* studies had been determined earlier [9-13]. However it was important in phase 1 to determine how these limits needed to be adjusted to define the 'strike zone' for *in vivo* measurements.

Specifically, the *in vitro* tests indicated that a possible criterion for determining if a shock had been 'effective' in targeting and fragmenting the stone could be based on the requirement that $m_2 / m_1 > 0.4$ and $t_c \sim 300$ μs [9-13]. However shorter collapse times could be expected *in vivo* [14]. Therefore phase 1 of the clinical studies examined the validity and application of these 'rules' to the *in vivo* tests. In phase 1, a complete set of acoustic and clinical data was obtained in 30 of the 118 subjects recruited (see above). On the basis of these data it was decided to alter the *in vitro* 'rules' for *in vivo* use such that an 'effective' shock is defined as one in which both $0.40 < m_2 / m_1 < 0.8$ and $t_c > 100$ μs. These rules define the limits of the strike zone in Fig. 12.

From the preceding discussion, it might be expected that the 'successful' treatments would tend to generate echoes which cluster in this strike zone. To test this hypothesis, a 'gold standard' method (mentioned above) was required for assessing whether a treatment had been successful. This 'gold standard' judgment was arrived at through use of a treatment score, CTS_2, which was provided by the consultant urologist at the 3-weeks patient's follow-up appointment. The CTS_2 score was taken to be the 'gold standard' since the clinical decision on the need for further treatment was based on this. To obtain CTS_2, a form was devised (see Leighton *et al.* [13]) which guided the urologist to base the treatment score for this study on the X-ray images alone. In assessing the need for further treatment, the urologist may in fact take into account other data available at the three-week follow-up (e.g. any reduction in the sensation of pain, comments by the patient on the passing of stone fragments). However, these issues were not used in our study to provide the treatment score CTS_2, as the comparisons involving the latter required an objective and quantitative measure. As a result, the form was designed such that the clinician used only the X-ray image when providing CTS_2.

The judgment of the radiographer immediately at the end of treatment was used to provide the other clinical treatment score CTS_1 - this score was not treated as a 'gold standard' but simply used to compare the judgments of the radiographer at the end of treatment, with the CTS_2 judgment of the urologist at the three-week follow-up. The form for CTS_1 was also designed so that only the X-ray image was used to inform this treatment score.

Details of the forms and the methods used to collect CTS_1 and CTS_2 from the clinicians are given in Leighton *et al*. [13]. Both clinicians use a six point scale of clinical treatment scores (0-5) based on the degree of stone fragmentation (and made without knowledge of the output of the passive acoustic system). They were qualitatively judged by the lithotripter operator, from the X-ray at the end of the treatment (CTS_1), and at the three week follow-up appointment (CTS_2) by a urologist, with '0' indicating no fragmentation, '3' indicating 50% fragmentation and '5' complete fragmentation..

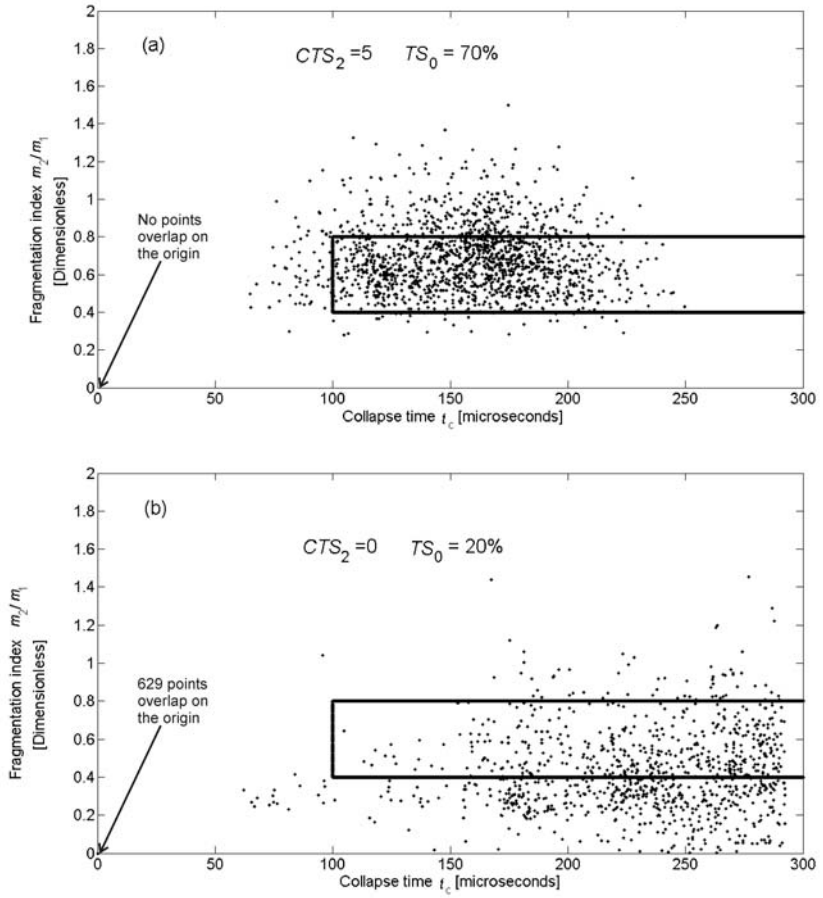

FIGURE 12. Plots from phase 1 of the clinical study giving the values of the acoustic parameters m_2 / m_1 and t_c for each shock from two sample treatments. The first plot (a) is for a 'successful' treatment, as classified by the clinician from the X-rays (CTS_2 =5); the second plot (b) is for an 'unsuccessful' treatment as classified by the clinician from the X-rays (CTS_2 =0). The area delimited by the solid line ($0.4< m_2 / m_1 <0.8$ and $t_c >100$ μs) represents the semi-empirical rules that appear from the phase 1 study to give the optimum indication of 'effective' and 'ineffective' shocks. It is postulated from the phase 1 study that a large number of 'effective' shocks (i.e. falling within the solid lines) result in a 'successful' treatment. Note that whilst Fig. 12(a) contains no points at the origin, Fig. 12(b) contains 629 overlapping points at the origin (see the Methods section for explanation; further details can be found in Leighton *et al.* [13]). Figure reproduced with permission from reference [13], where it previously appeared: *Ultrasound in Medicine and Biology* doi:10.1016/j.ultrasmedbio.2008.03.011 in press (by T. G. Leighton, F. Fedele, A. J. Coleman, C. McCarthy, S. Ryves, A. M. Hurrell, A. de Stefano, and P. R. White) "A device for monitoring the efficacy of ESWL using passive acoustic emissions, Copyright Elsevier 2008.

Examination of the data for the two patients shown in Fig. 12 reveals that, as expected, the successful treatment (Fig. 12(a), judged successful because this treatment was awarded CTS_2 =5) indeed shows greater clustering of points within the strike zone than occurs with the unsuccessful treatment (Fig. 12(a), for which CTS_2 =0). Note also that the process by which the algorithm places particularly

'unsuccessful' points on the origin, detected no such points in the 'successful' treatment of Fig. 12(a), but detected 629 such points for the 'unsuccessful' treatment of Fig. 12(b).

The second goal of the phase 1 study was to assess what proportion of the shocks in a given treatment need to be 'effective' for the treatment as a whole to be judged as being 'successful' by the acoustic system. The percentage of shocks at the end of a treatment which fell into the strike zone was termed TS_0, and the treatments of Fig. 12(a) and 12(b) exhibited TS_0 =70% and 20% respectively. In consultation with the clinicians, it was decided that the comparison between the different treatment scores should be based on a bi-modal verdict (in that $CTS_2 \geq 3$ could be termed a successful treatment, and $CTS_2 < 3$ indicated an unsuccessful treatment). Given this protocol, the critical value for TS_0 to divide between successful and unsuccessful treatments was assessed to be 50%, such that scores of $TS_0 \geq 50\%$ can be usefully classified as 'successful' (see Leighton *et al*. [13] for details of the reasoning). This hypothesis was tested in the Phase 2 clinical study.

Phase 2 clinical study

Having in phase 1 defined the rules by which the strike zone is delineated ($0.40 < m_2 / m_1 < 0.8$ and $t_c > 100\ \mu s$), and the threshold value of TS_0 which will be used to judge whether the acoustic sensor considers the treatment to have been successful (TS_0 =50%), the phase 2 clinical study proceeded to test these criteria on 49 of the 85 subjects that were originally recruited. The increased capture rate (59% of the original 85, compared to 25% of the 118 patients who consented to take part in phase 1) reflects a greater robustness of the equipment and a greater familiarity of the nurse with the system. In fact, one reason why only a proportion of shocks in a given treatment were captured arose because, when the operator changed the setting on the lithotripter, the nurse manually had to enter the new setting into the recording software, a task which resulted in some loss of data (and which could be avoided if the device were to be interfaced with the ESWL to detect the setting automatically).

The recording software consisted of a custom-made SEAC (Secondary Emissions Analysis in Clinic) interface. Although the Ethics approval for this clinical work only allowed comparison of the final TS_0 score against the CTS_2 gold standard score given 3 weeks after treatment, the SEAC software provided a real-time display which showed: (i) a cumulative indication of the success of the therapy delivered at any point during a single treatment session (the score $TS(t)$, the proportion of shocks so far in a treatment which were 'effective', and which equals TS_0 at the end of the treatment); and (ii) several features that reflect the ongoing acoustic verdict of the performance of each shock as it is delivered. Several of the latter are featured in Fig. 13, which is a

screen shot[1] of the SEAC output, with dashed lines added to facilitate the explanation. These dashed lines divide the screen shot into boxes, numbered (1) to (5).

The SEAC software allows storage of patient identification details (Box 1) and control of the waveform capture via oscilloscope settings (Box 2). Waveform acquisition is triggered from the electromagnetic pickup detected on the generation of each shock, and the 'Analysis start time' slider in Box 2 ensured that there was sufficient delay after triggering to eliminate the electromagnetic signal from the analysis. The lithotripter source power level or setting is manually entered, and displayed in Box 2 along with a virtual red/green 'traffic-light' indicator at the bottom right-hand corner of Box 2. This light is automatically updated after every shock to provide the ESWL operator with real-time feedback as to whether the previous shock has been effective, so that for example a sustained red display in this indicator could prompt the operator to consider re-targeting the stone.

Box 3 in Fig. 13 was included to allow additional digital filtering of the data either to improve the signal to noise ratio or to look only at specific frequency components. This option was disabled for the current study. Box 4 records a count of the number of shocks administered and information on software-equipment synchronisation. A *Test On* button (in Box 4) allowed the software to run in test mode (i.e. without saving any data), to check the appropriate settings to use for the specific treatment before starting the acquisition and storage of large quantities of data in the form of voltage waveforms for each shock. The *Start* button began the acquisition of data, and is replaced by a *Stop* button during acquisition.

The end-of-treatment quantitative treatment score (TS_0) is shown in the pop-up window (Box 5). In addition, the graph on the lower left of the screen in Fig. 13 shows the waveform captured by the passive acoustic sensor from each shock. It provides a visual clue to the operator as to the ongoing functioning of the acoustic system. The two graphs stacked one-above-another on the lower right of the screen in Fig. 13 plot the single-shock values of m_2/m_1 (upper panel, open circles) and t_c (lower panel, grey crosses) as a visual guide to trends in the effectiveness of a set of shocks. To reiterate a key point, ethics permission would not allow these real time indicators of the effectiveness of the treatment to be communicated to the therapist, and assessments of the equipment performance could only be made by comparing the acoustic score at the end of the treatment (TS_0) with the gold standard delivered three weeks later by the urologist.

This comparison was undertaken in phase 2, using the rules derived in phase 1 (that the strike zone is defined by $0.40 < m_2/m_1 < 0.8$ and $t_c > 100$ μs, and that the acoustic results indicate a successful treatment if $TS_0 \geq 50\%$). The second clinical study (Phase 2) demonstrated almost perfect agreement (kappa=0.94) between the number of 'successful' treatments, defined as greater than 50% fragmentation as determined by

[1] A movie of the software running is available at the web site http://www.isvr.soton.ac.uk/fdag/Litho_07/litho_07(main).htm and at the *Ultrasound in Medicine and Biology* website (http://www.umbjournal.org), on the page associated with reference [13].

X-ray at the follow-up appointment, and the device-derived global treatment score, TS_0. The acoustic system is shown to provide a test of the 'success' of the treatment that has a sensitivity of 91.7% (in that the acoustic device identified $TS_0 \geq 50\%$ for 11 of the 12 treatments for which $CTS_2 \geq 3$) and a specificity of 100% (in that the acoustic device gave $TS_0 < 50\%$ for all of the 37 treatments for which $CTS_2 < 3$). In contrast, the degree of agreement between the two clinical scores CTS_1 and CTS_2 was similar to that found in phase 1. This level of agreement was quantified in this case by kappa=0.38.

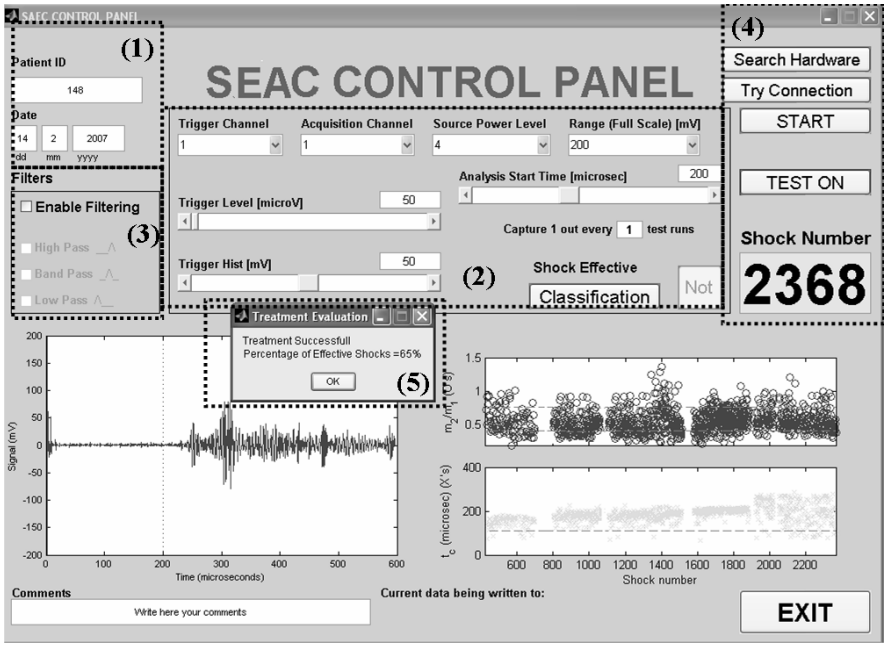

FIGURE 13. A screen shot of the output of the SEAC software interface used by the ESWL operator during phase 2 of the project. The dotted lines demarcating numbered boxes have been added to identify areas in the display (see text for details). Box 5 gives an indication of the percentage of the 2368 shocks given in this treatment which were effective at damaging the stone (TS_0). A score here of 65% indicates a successful treatment. The values of the acoustic parameters (m_2/m_1 and t_c) for each shock are shown in the graphs on the bottom right hand side of the interface, allowing trends to be noted. The bottom left panel plots the echo time history of the most recent shock, to allow assessment of the extent to which it conforms with the expected structure (noting however from Leighton *et al.* [13] that visual inspection is not as reliable at spotting two-burst structures as plots of the energy time history). In addition to these, there are three other display outputs from SEAC, and these are particularly important. The first of these is the treatment score TS_0 obtained at the end of the treatment (Box 5, described above); the second is the cumulative ratio $TS(t)$ of effective shocks to the total number of shocks given from the start of the treatment to any point during it (which equals TS_0 at the end of treatment); the third indicator is the red/green indicator light which provides feedback on the most recent shock. Trends in these are available (e.g. via the two graphs on the bottom right of the screen). Figure reproduced with permission from reference [13], where it previously appeared: *Ultrasound in Medicine and Biology* doi:10.1016/j.ultrasmedbio.2008.03.011 in press (by T. G. Leighton, F. Fedele, A. J. Coleman, C. McCarthy, S. Ryves, A. M. Hurrell, A. de Stefano, and P. R. White) "A device for monitoring the efficacy of ESWL using passive acoustic emissions, Copyright Elsevier 2008.

Monitoring the effects of respiration

It has previously been suggested [22, 23] that the depth of respiration could affect the clinical outcome. The device was used to demonstrate *in vivo* the sensitivity of the passive acoustic sensor to factors that influence targeting. The study is detailed in Leighton *et al.* [13].

Passive acoustic monitoring could possibly be used to provide a real-time check the effectiveness of a system which is designed to use respiration as a trigger for shock production in order to improve targeting, as issue which may be more critical for devices which use small foci rather than wide focus lithotripters [24].

CONCLUSIONS

This paper describes the sequence of studies that led to the first passive acoustic detector for the efficacy of ESWL treatment, which has been proven in clinical trials. The scope of the ethical approval did not allow the output of the sensor to be communicated in theatre to the clinicians. Therefore, we were prevented from testing whether the use of the device affects re-treatment rates. However the study has indicated the clinical usefulness of this technology: in the phase 2 study, the end-of-treatment score (automatically provided in real time by the device) correlated well with the judgment of the consultant urologist given at the patient's 3-week follow-up (kappa=0.94). In particular, this correlation is much better than that between the judgement of the urologist and the end-of-treatment opinion of the radiographer (kappa=0.38 in phase 2). In addition, for the 49 treatments in the second clinical study, the passive acoustic device demonstrated a sensitivity of 91.7% and a specificity of 100%.

The passive acoustic detector provides feedback from acoustic signals *within the patient* as to the interaction between the shock and the tissue. Such passive monitoring offers a range of benefits. At the simplest level, it monitors whether the shock enters the body or whether the shock amplitude reaching the tissue has been degraded, e.g. as a result of poor coupling or loss of coupling (through loss of contact, or bubble formation in the coupling gel). Perturbations on the treatment can be monitored in real time (the example of ventilation has been studied with this device). The current manifestation of the device was designed to be simple and robust: a single unfocused receiver is required, which is robust with respect to use (e.g. placement of the patient), and the operation and the verdict of the device are automatically computed. The data for the clinical studies reported here were obtained by a nurse operating the device. Further discussions of the implications of this technology are given in reference [13].

ACKNOWLEDGMENTS

The Engineering and Physical Sciences Research Council provided a grant from 2000 to 2003 (EPSRC grant, GR/N19243/01, Principle Investigator: TG Leighton; Co-Investigator: AJ Coleman), which was followed by a further grant from 2005 to 2006 (Grant ref: EP/D503310/1; Principle Investigator: TG Leighton; Co-Investigator: AJ Coleman). However over this seventeen-year project, much of the work was undertaken without sponsorship (the average annual income to cover all costs was less than £20k). As such the project relied heavily on the generous donation of equipment and services from a range of munificent sources. From the partner company Precision Acoustics Ltd., T. Gill and D. Bell provided invaluable assistance in developing the passive sensor. R. Tiptaft, J. Glass, D. Phillips and T. Jessop (Urology Department at Guy's and St Thomas' NHS Trust) are gratefully acknowledged for their support during the clinical study. C. McKinnon (Centre for Enterprise and Innovation, University of Southampton) and T. Parlett (Intellectual Property Officer, Guy's & St Thomas' NHS Trust) are thanked for their work in the contractual and commercial aspects of this study. From ISVR, D. Finfer is thanked for assistance in software programming, G. T. Yim is thanked for his advice on computing hardware, and V. Humphrey is thanked for loan of interim replacement transducers and preamplifiers when the apparatus was sent for servicing. NHS Innovations London were kind enough to shortlist the device for their award. All clinical work was approved by the local research ethics committee of Guy's and St Thomas' NHS Foundation Trust.

REFERENCES

1. A. J. Coleman, M. J. Choi, J. E. Saunders and T. G. Leighton, *Ultrasound Med. Biol.* **18**, 267-281 (1992).
2. A. J. Coleman, M. Whitlock, T. G. Leighton, and J. E. Saunders, *Physics in Medicine and Biology* 38, 1545-1560 (1993).
3. T. G. Leighton, *The Acoustic Bubble*. Academic Press, London, 1994, pp. 458-463.
4. K. B. Cunningham, A. J. Coleman, T. G. Leighton, and P. R. White, *Acoustics Bulletin* **26**, 10-16 (2001).
5. T. G. Leighton, *International Journal of Modern Physics B*, **18**, 3267-314 (2004).
6. A. R. Jamaluddin, G. J. Ball, and T. G. Leighton, "Free-Lagrange simulations of shock/bubble interaction in shock wave lithotripsy," in *Proceedings of the Second International Conference on Computational Fluid Dynamics, ICCFD,* Sydney, Australia, 2002, pp. 541-546.
7. C. K. Turangan, A. R. Jamaluddin, G. J. Ball, and T. G. Leighton, *Journal of Fluid Mechanics*. **598**, 1-25 (2008).
8. T. G. Leighton, **"**From seas to surgeries, from babbling brooks to baby scans: Bubble acoustics at ISVR," in *Proceedings of the Institute of Acoustics*, **26**(1), 357-381 (2004).
9. F. Fedele, A. J. Coleman, T. G. Leighton, P. R. White and A. M. Hurrell, "Development of a new diagnostic sensor for extra-corporeal shock-wave lithotripsy", in *Proceedings of the First Conference in Advanced Metrology for Ultrasound in Medicine, Journal of Physics: Conference Series* **1**, 134-139 (2004).

10. F. Fedele, A. J. Coleman, T. G. Leighton, P. R. White and A. M. Hurrell, "Development of a new diagnostic device for extracorporeal shock-wave lithotripsy", in *Proceedings of the X Mediterranean Conference on Medical and Biological Engineering "Health in the Information Society"*, Paper No. 54, 4pp (2004).
11. F. Fedele, "Acoustic sensing of renal stones fragmentation in extracorporeal shockwave lithotripsy", PhD thesis, University of Southampton (2008).
12. T. G. Leighton, F. Fedele, A. Coleman, C. Mccarthy, A. R. Jamaluddin, C. K. Turangan, G. J. Ball, S. Ryves, A. Hurrell, A. De Stefano and P. R. White, "The development of a passive acoustic device for monitoring the effectiveness of shockwave lithotripsy in real time", in *Proceedings of the 7th European Acoustics Association International Symposium on Hydroacoustics*, **11**, 159-180 (2008).
13. T. G. Leighton, F. Fedele, A. J. Coleman, C. McCarthy, S. Ryves, A. M. Hurrell, A. de Stefano, and P. R. White, "A device for monitoring the efficacy of ESWL using passive acoustic emissions," *Ultrasound in Medicine and Biology* (in press), 2008, doi:10.1016/j.ultrasmedbio.2008.03.011.
14. P. Zhong, I. Cioanta, F. H. Cocks and G. M. Preminger, *J. Acoust. Soc. Am.* **101**(1), 2940–2950 (1997).
15. R. O. Cleveland, O. A. Sapozhnikov, M. R. Bailey and L. A. Crum, *J. Acoust. Soc. Am.* **107**(3), 1745-1758 (2000).
16. T. J. Matula, P. R. Hilmo, M. R. Bailey and L. A. Crum, *Ultrasound Med. Biol.* **28**(9), 1199-1207 (2002).
17. M. R. Bailey, Y. A. Pishchalnikov, O. A. Sapozhnikov, R. O. Cleveland, J. A. McAteer, N. A. Miller, I. V. Pishchalnikova, B. A. Connors, L. A. Crum and A. P. Evan, *Ultrasound Med. Biol.* **31**(9), 1245-1256 (2005).
18. N. R. Owen, M. R. Bailey, L. A. Crum, O. A. Sapozhnikov and L. A. Trusov, *J. Acoust. Soc. Am.* **121**, EL41–EL46 (2007).
19. N. R. Owen, O. A. Sapozhnikov, M. R. Bailey, L. A. Trusov and L. A. Crum, "A passive technique to identify stone comminution during shock wave lithotripsy", in *Renal stone disease, Proceedings of the First Annual International Urolithiasis Research Symposium (ed. A. P. Evan, J. E. Lingeman, J. C. Williams Jr. AIP Conference Porccedings)*, pp. 364-367 (2007).
20. T. G. Leighton, A. J. Coleman, F. Fedele and P. R. White, A passive acoustic system for evaluating the in-vivo performance of extracorporeal shockwave lithotripsy, UK Patent Number 0319863.7 (2004).
21. F. Fedele, A. J. Coleman, T. G. Leighton, P. R. White and A. M. Hurrell, *Acoustics Bulletin* **29**, 34-39 (2004).
22. R. O. Cleveland, R. Anglade and R. K. Babayan, *J. Endourol.* **18**(7), 629-633 (2004).
23. M. A. Warner, M. E. Warner, C. F. Buck, J. W. Segura, *J. Urol.* **139**(3), 486-487 (1988).
24. W. Eisenmenger, X. X. Du, C. Tang, S. Zhao, Y. Wang, F. Rong, D. Dai, M. Guan and A. Qi, *Ultrasound Med. Biol.*, **28**(6), 769-774 (2002).